MAGNETIC RESONANCE IN CHEMISTRY
Magn. Reson. Chem. 2007; **45**: 865–877
Published online in Wiley InterScience
(www.interscience.wiley.com) DOI: 10.1002/mrc.2060

MRC

An NMR, IR and theoretical investigation of ^{1}H Chemical Shifts and hydrogen bonding in phenols†

Raymond J. Abraham[1] and Mehdi Mobli[2]*

[1] Chemistry Department, The University of Liverpool, Liverpool L69 3BX, UK
[2] Manchester Interdisciplinary Biocentre, University of Manchester, Manchester M17 ND, UK

Received 16 May 2007; Revised 18 June 2007; Accepted 21 June 2007

The change in ^{1}H NMR chemical shifts upon hydrogen bonding was investigated using both experimental and theoretical methods. The ^{1}H NMR spectra of a number of phenols were recorded in $CDCl_3$ and DMSO solvents. For phenol, 2- and 4-cyanophenol and 2-nitrophenol the OH chemical shifts were measured as a function of concentration in $CDCl_3$. The plots were all linear with concentration, the gradients varying from 0.940 (phenol) to 7.85 (4-cyanophenol) ppm/M because of competing inter- and intramolecular hydrogen bonding. *Ab initio* calculations of a model acetone/phenol system showed that the OH shielding was linear with the H···O=C distance (R) for $R < 2.1$ Å with a shielding coefficient of −7.8 ppm/Å and proportional to $\cos^2\varphi$ where φ is the H···O=C−C dihedral angle. Other geometrical parameters had little effect. It was also found that the nuclear shielding profile is unrelated to the hydrogen bonding energy profile. The dependence of the OH chemical shift on the π density on the oxygen atom was determined as *ca* 40 ppm/π electron. This factor is similar to that for NH but four times the value for sp^2 hybridized carbon atoms. The introduction of these effects into the CHARGE programme allowed the calculation of the ^{1}H chemical shifts of the compounds studied. The CHARGE calculations were compared with those from the ACD database and from GIAO calculations. The CHARGE calculations were more accurate than other calculations both when all the shifts were considered and also when the OH shifts were excluded. The calculations from the ACD and GIAO approaches were reasonable when the OH shifts were excluded but not as good when all the shifts were considered. The poor treatment of the OH shifts in the GIAO calculations is very likely due to the lack of explicit solvent effects in these calculations.

KEYWORDS: NMR; ^{1}H; chemical shifts; phenols; IR; CHARGE; GIAO; DFT; hydrogen bonding

INTRODUCTION

Nuclear magnetic resonance (NMR) is now the major technique used to solve structural problems of organic and bio-molecules in solution. This, however is critically dependent on the correct assignments for the NMR spectrum. ^{1}H chemical shifts are still often estimated from various empirical tables.[1,2] These work well for rigid, particularly planar aromatic molecules but are much less accurate for complex flexible molecules as they are independent of the three-dimensional structure of the molecule. Although much progress has been made in this area for ^{13}C predictions (see for example the work of Kishi[3]), these are not generally applicable to ^{1}H chemical shifts. *Ab initio* calculations are, in principle, ideal for such calculations but they are very much dependent on geometry, basis set and solvent interactions. Thus, the total calculation time for a thorough investigation renders these methods inaccessible for routine use. The computationally less demanding molecular mechanics or semi-empirical methods are today routinely used in structure calculations.[4,5] These can rapidly compute multiple conformations of a molecule and thus sample the conformational space (energy profile) efficiently in contrast to the local minima found by *ab initio* calculations. This approach has recently found considerable commercial interest in NMR chemical shift calculations (i.e. NMRPredict, Perch).[6,7] This method can provide chemical shifts of an ensemble of structures which are then averaged (according to the Boltzmann distribution) to predict the observed ^{1}H NMR spectrum. Although this method has found applications in routine spectral assignment its utility in studying molecular interactions has so far not been investigated. One of the largest ^{1}H chemical shift changes upon interaction is due to hydrogen bonding. Although considerable literature exists in this field, the very definition of a hydrogen bond, beyond being a proton covalently bound to an electronegative atom interacting with another electronegative atom, is somewhat diffuse. The literature is sometimes conflicting[8] and it is apparent that no simple definition exists and each case must be analysed independently.[9] We wish to study hydrogen bonds from a chemical shift point of view to obtain a semi-empirical

*Correspondence to: Mehdi Mobli, Manchester Interdisciplinary Biocentre, University of Manchester, Manchester M17 ND, UK.
E-mail: mehdi.mobli@manchester.ac.uk
†This is part 25 of ^{1}H Chemical Shifts in NMR series.

MRC

method which will describe the hydrogen bond and its effect on the ^{1}H chemical shift for intra- and intermolecular H-bonds. Here, we use phenols as the model system, as they are biologically important and also provide a simple model where several interactions can be studied simultaneously. We will investigate the geometrical dependence of the H-bonded proton chemical shift by both experimental and *ab initio* methods to determine whether this can be simulated with existing models,[10] or whether a specific term needs to be included to satisfy the observed data. The theoretical justification of such a term will also be discussed.

Both inter- and intramolecular H-bonding in phenols has been investigated for many years with IR and NMR being the major tools for investigating these H-bonds in solution.[11–14] The OH chemical shift of phenol varies from 4.6δ in dilute $CDCl_3$ to 9.2δ in d_6-DMSO[15] because of intermolecular H-bonding in DMSO. In contrast, the chemical shifts of the OH protons of 2-hydroxybenzophenones are insensitive to changes in both temperature and concentration in CCl_4 because of a strong intramolecular H-bond impeding the formation of intermolecular H-bonds.[16] The OH bond weakens and H-bond length increases[17–21] on and this produces a decrease in the OH stretching frequency and a large deshielding of the OH proton chemical shift.[22,23] Indeed, these effects were found to be correlated for intramolecularly hydrogen-bonded molecules.[18,24,25] The majority of the early studies were aimed at determining the hydrogen-bond energy for the weakly H-bonded systems such as *ortho* halophenols (excluding stronger interactions as in 2-hydroxyacetophenone). These early results have been reviewed[26] and an intramolecular H-bond energy of 2.5–3.5 kcal/mol is suggested.

CNDO/2[27] and *ab initio*[28] calculations showed that the OH frequencies correlated well with calculated OH bond lengths and agreed well with the *ab initio* calculated values. For intramolecular H-bonds, the electron density at the bond critical point (BCP)[29] could be correlated to the H-bond energies.[30] This gave a method of combining *ab initio* and AIM calculations.[31,32] The H-bond energy in malonaldehyde was calculated by this method to be *ca* 10 kcal/mol, and in derivatives of 2-(*N*-dimethyl aminomethyl)phenols *ca* 8–9 kcal/mol. This agrees well with the earlier dilution experiments, confirming the presence of a stronger interaction.[16]

Lampert *et al*.[33] used GIAO theory at the HF and B3LYP level to calculate ^{1}H, ^{13}C and ^{17}O chemical shifts in phenol and 2-hydroxybenzoyl compounds. HF calculations produced poor results for the hydrogen-bonded systems. The B3LYP calculations gave results agreeing better with the experimental values, but the calculated OH chemical shift in salicylaldehyde still varied from 9.3 to 13.0 δ (*cf* experimental 11.02 ppm) depending on the basis set used. Bagno[34] compared different theoretical approaches for calculating nuclear shielding with experimental results and found the B3LYP/cc-pVTZ and B3LYP/6-31G(d,p) levels to give the best agreement.

Here, we have used the phenols shown in Table 1 (*cis* and *trans* conformations of these phenols are shown in Fig. 1) to study both intra- and intermolecular hydrogen bonds by ^{1}H NMR in $CDCl_3$ and DMSO solution and by IR measurements. We wish to determine whether the ^{1}H chemical shifts in these compounds, including the OH proton, can be calculated using a semi-empirical approach. We have used the CHARGE programme which calculates proton chemical shifts based on atomic charges, electric field, steric and anisotropy effects.[35] The programme now includes all the common functional groups in organic chemistry. The programme has been extended to calculating OH chemical shifts in alcohols and in *ortho* substituted phenols with strong intramolecular H-bonds (e.g. 2-hydroxybenzaldehyde, 2-hydroxyacetophenone, 2-nitrophenol and methyl salicylate) with OH···O distances shorter than 2.0 Å. In the latter compounds, the large deshielding effect of the *ortho* substituent on the OH proton was reproduced in CHARGE by an r^{-12} function to give moderate agreement with the observed shifts when studying aromatic carbonyl compounds.[36] We now wish to refine this important term using a DFT approach. This study will include the investigation of the orientation dependence of the H-bond on the chemical shift (*cf* those found for $^2J_{(N,N)}$ coupling constants[37,38]). The observed shifts in the phenols studied can then be compared with those calculated by CHARGE and also with both *ab initio* (GIAO) and database (ACD) approaches.

RESULTS AND DISCUSSIONS

Theoretical analysis

In this section *ab initio*, calculations used to provide insight into the shielding of the OH proton in a hydrogen bond are discussed. The C═O···H–O hydrogen bond arises from the overlap of the lone pairs of the oxygen with the s-orbital of the hydrogen atom and this is maximum for a linear O: H–O system. In molecular mechanics energy calculations,

Table 1. *Ortho* (–X) and *para* (–Y) substituted phenols used

Phenol	–X	–Y
[1]	H	H
[2]	F	H
[3]	Cl	H
[4]	Br	H
[5]	I	H
[6]	Me	H
[7]	OMe	H
[8]	CN	H
[9]	CF_3	H
[10]	NO_2	H
[11]	$COOCH_3$	H
[12]	H	CN
[13]	H	F
[14]	H	t-Bu
[15]	H	NO_2
[16]	H	CF_3
[17]	H	Ome
[18]	Cl	Cl
[19]	CHO	H
[20]	$COCH_3$	H

DOI: 10.1002/mrc

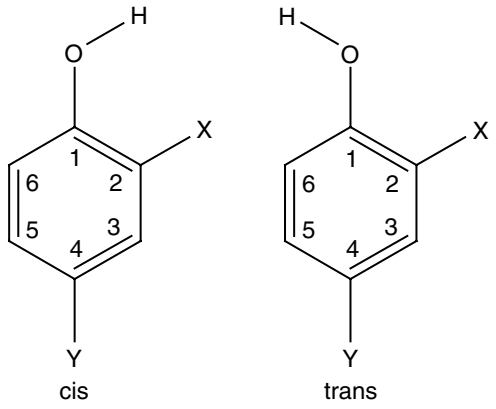

Figure 1. *Cis* and *trans* conformations of 2(−X), 4(−Y) substituted phenols.

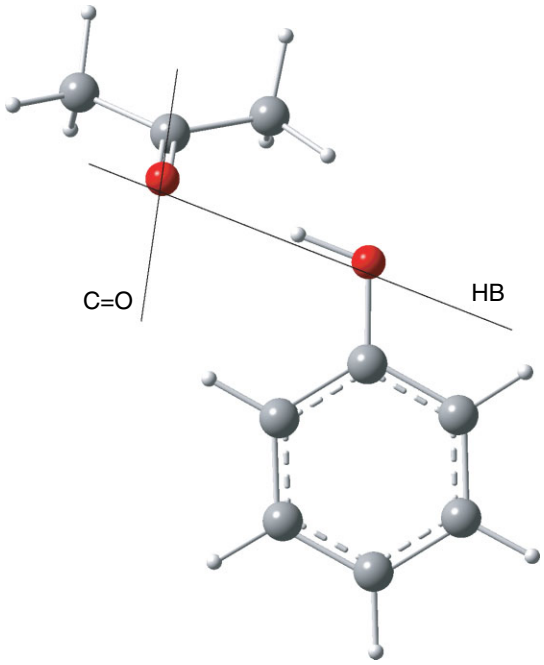

Figure 2. *Ab initio* optimization of the acetone–phenol interaction.

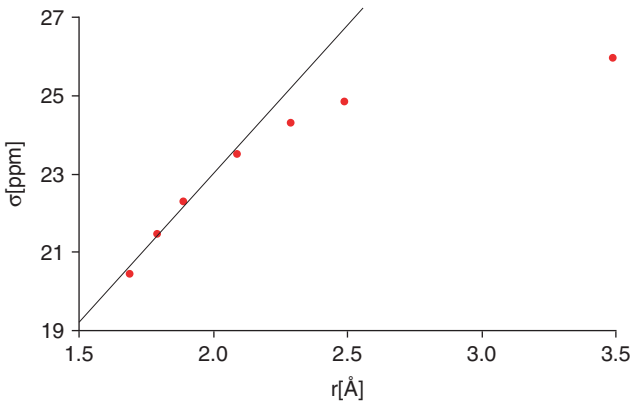

Figure 3. The distance (OH···O) dependence of the chemical shift of the OH proton of phenol hydrogen bonded to acetone. Best fit to a linear function for data below 2.1 Å is also plotted. The minimum energy distance was found to be 1.7 Å.

hydrogen-bonding interactions are treated separately.[4,39] They are usually described by a Lennard-Jones 6–12 or 10–12 potential plus an angle dependence so that the orientation dependence of the preferred geometry is simulated. Cut-off values for hydrogen bonds are also sometimes used. We wish to determine both the distance dependence and any angle dependence of the chemical shifts in the H-bond.

The following procedure was used to model the hydrogen-bonding interaction between acetone and phenol. A molecular mechanics force field (MM2) was used to find the optimum arrangements of the two molecules. These were then minimized using DFT (B3LYP) with a small basis set (3–21G), which also was used to calculate the electron populations. The nuclear shielding calculations (GIAO) were performed using the B3LYP/6–31+G(d,p) method. The calculations were performed for the acetone/phenol and DMSO/phenol systems. We consider here only the acetone/phenol results. The DMSO/phenol results are presented elsewhere.[40]

The minimum energy conformation for the acetone/phenol system is shown in Fig. 2 and this conformation has the planar acetone molecule orthogonal to the phenol ring plane. The nuclear shielding of the H-bonded proton was then calculated as a function of the distance between the interacting atoms of OH and ═O along the HB axis of Fig. 2 and is shown in Fig. 3.

Figure 3 shows a dramatic increase in nuclear shielding as the OH···O distance increases. Beyond 2–2.5 Å, the increase in nuclear shielding is comparably moderate. For distances less than or equal to 2.1 Å, the plot is almost linear. The correlation coefficient (R^2) for acetone using a linear function up to 2.1 Å is 0.98. Therefore the nuclear shielding due to the hydrogen bond for distances <2 Å may be accurately reproduced by a linear equation. This is both novel and important as at present ^{1}H chemical shifts of hydrogen-bonded systems, in which the hydrogen bond distance is less than 2 Å, are poorly predicted using classical models of anisotropy, electric field and steric effects alone (e.g. in the CHARGE programme). The implementation of this result will be applied later. The analogous DMSO/phenol calculations gave a very similar plot showing that this result is a general one. Ishikawa *et al.*,[41] when studying the substituent effects on the NH chemical shift in the NH···N system, stated that a change in chemical shift of *ca* 0.6 ppm was not due to changes in conformation as these changes were <0.05 Å (N···N distance in a NH···N hydrogen bond). Although the NH···N bond may not have a distance dependence such as that found in the OH···O case, our results suggest that at these distances small changes in conformations may indeed significantly contribute to changes in chemical shifts. In the OH···O case, above the corresponding change in distance would result in a change of 0.4 ppm, which can be regarded as a very significant contribution.

Increasing the angle between the OH and C═O bonds without changing any other parameters has a small linear deshielding effect on the OH proton (not shown) from 20.5 ppm at 100° to 21.0 ppm at 180°. To further investigate this effect, the nuclear shielding of a methane proton was

DOI: 10.1002/mrc

MRC

calculated on the approach of an acetone molecule in exactly the same way as the acetone/phenol calculations. Again here, a small deshielding effect (0.24 ppm) was found when the angle is changed from 113 to 180°. These results suggest that this angle has no major effect on the chemical shift of hydrogen-bonded OH protons. This is surprising since the hydrogen bond would be weakened in such an orientation (because of non-ideal overlap of orbitals). It should however be noted that the energy profile of the hydrogen bond may not necessarily follow the change in nuclear shielding. In fact, the change in nuclear shielding and energy between the methane–acetone and phenol–acetone complexes is very different. In the methane–acetone case, a deshielding of the C–H proton is found, but there is an overall decrease of 4 kcal/mole in the energy of the system when the C═O···H–C system is linear. In the phenol–acetone system, the same deshielding effect is found but an overall increase in energy (+2 kcal/mole) occurs when the same change in conformation is imposed (as the energetically favourable interaction with the lone pair of the oxygen is broken). This is a very significant result as often the increased deshielding of a proton is automatically interpreted as stronger hydrogen bonds.

In order to see if the hydrogen bond is sensitive to a change in the O–H···O angle, the change in chemical shift as a function of this angle was also calculated (keeping all other variables constant). Again, this results in an almost linear plot (not shown) with a slight decrease in the shielding from 20.9 to 20.5 ppm when the angle increases from 140 to 180°. There is only a small dependence of the nuclear shielding on this parameter.

The only other angle to investigate is the Me–C═O···H dihedral angle. As in the case of the C═O···H angle, changing this dihedral angle should result in the reduction of the orbital overlap of the C═O oxygen lone pair and the OH hydrogen, which again can be interpreted as weakening the hydrogen bond.

In contrast to the other angles, a dramatic change in chemical shift is noted as the dihedral angle is changed (Fig. 4). Thus, for an sp^2 hybridized oxygen (such as the C═O group) this dihedral angle has a significant effect on the nuclear shielding. Note that the plotted curve is essentially a $\cos^2 \varphi$ function. In the phenol/DMSO study, this angle was also found to be significant but the appearance of the curve is more in agreement with an sp^3 hybridized oxygen atom.[40]

The results show that the H–bond energy is not directly related to the nuclear shielding of the H–bonded hydrogen. The only significant factors influencing the nuclear shielding are the distance between the atoms involved in the hydrogen bond and the change in the R–X═O···H dihedral angle.

The above results are important in understanding non-bonded geometrical effects which influence the ^{1}H chemical shifts of OH protons. Bonded interactions based on partial atomic charges are already incorporated in the CHARGE programme; however, the effect of electron delocalization onto an oxygen atom in a π-system and the subsequent effect of this onto the ^{1}H chemical shift of the attached proton has not been investigated. This effect known as the π-shift is obviously of great interest when studying alcohols in aromatic systems, such as the phenols under

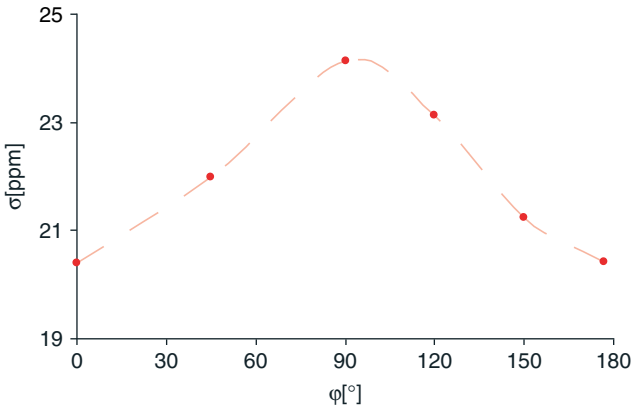

Figure 4. R–X═O···H dihedral angle (φ) dependence of the nuclear shielding of the OH hydrogen of phenol. The hydrogen bond acceptor is acetone.

investigation here. The corresponding effect for the carbon atom has however been studied in detail previously[42,43] and the same approach can be applied in determining this effect on the OH atom. This effect must thus be investigated prior to including the non-bonded geometrical effects studied above.

However, as the approach pursued here is a semi-empirical one, it is of paramount interest to use high quality experimental data in parameterizing the programme. We will therefore in the next section discuss the two major factors influencing the measured experimental data for alcohols, namely, concentration and solvent effects (temperature effects are neglected as all measurements are performed at room temperature). Both these effects involve complex intermolecular interactions which are much more difficult to model and calculate and this will be highlighted by studying these molecules for the hydrogen bonding in DMSO as solvent. Once these experimental influences are covered, we shall proceed to parameterize the π-shift and finally the geometrical effects illuminated by the *ab initio* studies in this section.

Concentration effects

IR spectra

In phenol, a sharp band at *ca* 3600 cm^{-1} is observed due to the free OH stretch (Fig. 5). For phenol, *o*-cresol, 2-CF_3-phenol, 2-cyanophenol and all 4-substituted phenols (except 2,4 dichlorophenol), additionally a broad band appeared at about 3450 cm^{-1} (Fig. 5(a)). When the concentration of phenol is decreased from 10 to 1 mg/ml, the broad band disappears, which indicates that this is due to intermolecular hydrogen bonding. The peak at 3700 cm^{-1} increases in intensity as the concentration is decreased and is due to the solvent. The IR spectrum of 2-cyanophenol was recorded at 1 mg/ml and also at 0.1 mg/ml. The broad band decreased in intensity relative to the sharp band, but was still present at 0.1 mg/ml concentration. Again, this broad band is attributed to the intermolecular hydrogen bonding of the OH group. The band due to the *trans* isomer at *ca* 3600 cm^{-1} was not observed for any of the compounds, in contrast to the spectra in CCl_4[11] and in the pure liquid.[13] This is not surprising as the *trans* isomer is of much higher energy in most cases

DOI: 10.1002/mrc

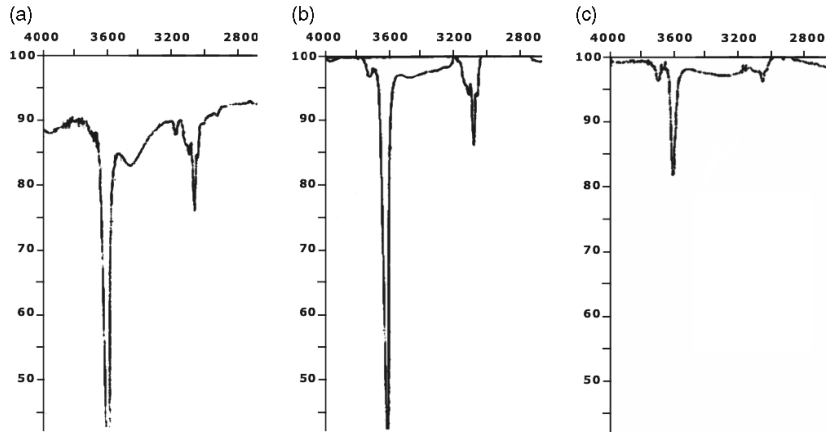

Figure 5. IR spectrum of phenol in $CDCl_3$ at (a) 10 mg/ml, (b) 5 mg/ml and (c) 1mg/ml.

Table 2. IR OH stretching frequency[a] of phenols in $CDCl_3$[b] and CCl_4, and as liquid with calculated energy differences ΔE(*cis* – *trans*)

Compound	$CDCl_3$	CCl_4			ΔE(*cis* – *trans*) (kcals/mol)
		Ref. 27	Ref. 28	Liquid Ref. 13	
Phenol	3605	3612	3611	3602	
2-Fluorophenol	3590		3591	3584	3.93
2-Chlorophenol	3548	3547	3546	3541	4.30
2-Bromophenol	3528		3528	3524	4.57
2-Iodophenol	3506		3505	3497	
2-Methylphenol (*o*-Cresol)	3610				−0.80
2-Methoxyphenol (Guaiacol)	3548	3558		3550	5.40
2-Cyanophenol	3568	3560			2.45
2-CF_3-phenol	3618				1.73
2-Nitrophenol	3258	3237		3256	
2-$COOCH_3$-phenol	3199				
4-Cyanophenol	3590	3597			
4-Fluorophenol	3607	3615		3607	
4-t-Bu-phenol	3607				
4-Nitrophenol	3590	3595			
4-CF_3-phenol	3599				
4-Methoxyphenol	3608				
2,4-Dichlorophenol	3546				
2-CHO-phenol	3189				
2$COCH_3$-phenol	3054				

[a] $\nu_{(OH)}$ given in cm^{-1}.
[b] Measured at a concentration of 10 mg/ml.

and as chloroform is a hydrogen bond donor the *cis* form could be more stabilized in this solvent than the *trans* form.

All the phenols studied gave the sharp free OH band (Table 2). The observed frequencies agree well with those reported earlier in CCl_4 solvent with the sole exception of the value for 2-nitrophenol. Note that only the 2-methyl and 2-CF_3 phenols have higher OH frequencies than phenol. In the 2-CF_3 phenol, a second OH band at 3699 cm^{-1} of lower intensity was observed probably because of a higher energy OH-*trans* conformation. This is supported by the *ab initio* calculations shown below.

For *ortho* chlorophenol ΔE (*cis* – *trans*) is 1.6 kcal/mol[11] (CCl_4), 2.4[13] (liquid) and 3.9[12] (vapour). To confirm these results, *ab initio* DFT calculations (B3LYP/6311++G (d,p)) were performed on some of the *ortho* phenols and this data is given in Table 2 together with the IR OH frequencies observed. The calculations confirm the much higher energy for the *trans* form in all the compounds except for 2-methyl substituted phenol in which the order is reversed and the 2-CF_3 substituted one, in which the energy difference is only 1.7 kcals/mol. These results confirm the structures of the *ortho* phenols which will be used for the NMR calculations.

NMR spectra

The OH proton chemical shift in phenol increases linearly with concentration of CCl_4 from 5.36 δ at infinite dilution to

DOI: 10.1002/mrc

6.98 δ for the saturated solution[25] (*ca* 120 mg/ml) at which point the OH chemical shift is constant and independent of concentration. This concentration dependence was attributed to a monomer–trimer equilibrium.[25,44] We measured the ^{1}H spectrum of phenol from 1 to 100 mg/ml ($\approx 0.01 - 1$ M) in $CDCl_3$. Again, the OH shift is linear with concentration Eqn (1) where c is the concentration in mg/ml. (correlation coefficient $R^2 = 0.999$).

The OH chemical shift of phenol in $CDCl_3$ changes only by 0.1 ppm with concentration change from 10 mg/ml to infinite dilution. As 0.1 ppm is the tolerated error in the chemical shift calculation, this concentration may be safely used in such predictions for weakly intermolecular H-bonded systems. For intramolecular H-bonds, the limit is much greater because of intramolecular interactions inhibiting any intermolecular H-bonding. For example, in *o*-bromophenol the OH chemical shift was independent of concentration. However, 2- and 4-cyanophenol and 4-nitrophenol showed intermolecular H-bonding even at very low concentrations and the concentration dependence of the OH chemical shift in these compounds is shown in Fig. 6 and Eqn (1). They all have correlation coefficients (R^2) of *ca* 0.99.

$$\begin{aligned} \text{Phenol} \quad & \delta_{(OH)} = 4.60 + 0.01c \\ \text{4-cyano} \quad & \delta_{(OH)} = 5.266 + 0.066c \\ \text{2-cyano} \quad & \delta_{(OH)} = 5.659 + 0.0486c \\ \text{4-nitro} \quad & \delta_{(OH)} = 5.356 + 0.0283c \end{aligned} \tag{10}$$

The gradients of the plots are 0.940, 3.96, 5.71 and 7.85 ppm/M for phenol, 4-nitro, 2-cyano and 4-cyano phenol. The gradients for the substituted phenols are all much larger than phenol illustrating the much stronger intermolecular H-bonding in these compounds.

It is of interest to note that the strong intermolecular hydrogen bonding can lead to misinterpretation of data. At 10 mg/ml, the *para* cyanophenol OH is clearly at a higher δ compared to that of the *para* nitrophenol, but at lower concentrations the situation is reversed, (as predicted by both CHARGE and GIAO calculations). Thus, for such compounds the calculated values of the OH protons should be used with caution as self-association is not accounted for. In Tables 3 and 4, the infinite dilution value of the OH shift is used to compare with the calculated values.

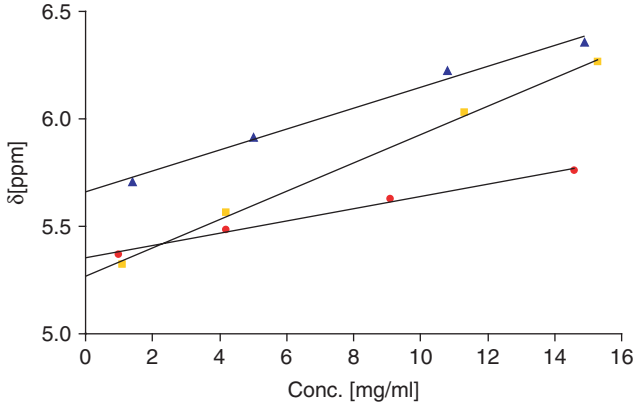

Figure 6. Concentration dependence of the self association of mono substituted phenols in $CDCl_3$ (4-NO_2 = circles, 4-CN = squares, 2-CN = triangles).

The intermolecular hydrogen bonding of the OH proton, which causes the concentration dependence of the OH chemical shift, is determined by a number of factors; the acidity of the OH proton, the hydrogen bonding ability of the substituent, steric hindrance of the OH proton by the substituent (for *ortho* substituted phenols), and the strength of any intramolecular hydrogen bond. The influence of these competing factors can be seen in 2-nitrophenol in which the intramolecular hydrogen bond dominates, impeding intermolecular hydrogen bonds, thus showing little concentration dependence. In contrast, in 2-cyanophenol the intermolecular hydrogen bond competes successfully with the intramolecular interaction giving a strong concentration dependence. In accordance with these findings, 4-cyanophenol having no intramolecular H-bonds shows the strongest concentration dependence. The equilibrium constant for the formation of the dimer of phenol and benzonitrile is 3.5 M^{-1}, compared with 7.6 M^{-1} for the complex of benzonitrile and 4-cyanophenol,[45] and this supports the above interpretation of the NMR data. Also, the chemical shift value of the OH proton of 2-cyanophenol is similar to that of the 2-Cl and 2-Br compounds. They have been shown[26,46] to be subjected to less self-association compared to phenol and to have the lowest equilibrium constants of the halophenols for the dimerization equilibrium.

Solvent effects (DMSO vs $CDCl_3$)

The multi-functional concentration dependence of the OH shift, discussed above, can be simplified by measuring the OH chemical shifts in dilute $CDCl_3$ and DMSO solvents. In DMSO, the OH proton is hydrogen bonded to the solvent, thus only the H-bonding ability of the OH proton is being measured. The ^{1}H chemical shifts of all the compounds investigated are given in $CDCl_3$ and DMSO solvents (Tables 3,4) and it is of interest to consider the differential solvent effect ($\Delta\delta = \delta(\text{DMSO}) - \delta(CDCl_3)$). A recent study[45] showed that $\Delta\delta$ for a protic hydrogen is directly related to the overall hydrogen bond acidity of the compound for a wide range of solutes, which included all the compounds in Fig. 6 and phenol. This is the first direct correlation between the proton chemical shift and a thermodynamic quantity.

These differential solvent shifts can be modelled using the formulation of the CHARGE programme. The largest value of $\Delta\delta$ is for the OH proton because of strong hydrogen bonding with the DMSO solvent and this value is typically 4.77 ± 0.4 ppm. (e.g. phenol δ (OH) is 9.29 (DMSO) *versus* 4.60 ($CDCl_3$). For intramolecularly hydrogen-bonding phenols, e.g. *o*-methoxyphenol, δ(OH) is 8.82 (DMSO) and 5.59 ppm ($CDCl_3$) and both the deshielding in $CDCl_3$ and the shielding in DMSO (compared to phenol) is clearly due to the intramolecular hydrogen bonding between the OH and the 2-OMe substituent.

For all other protons, the solvent induced effects are much less, but in general $\Delta\delta$ is negative. For example, for phenol$\Delta\delta$

DOI: 10.1002/mrc

Table 3. ^{1}H chemical shifts (δ) of *ortho* substituted phenols in $CDCl_3$ and DMSO together with calculated chemical shifts using various computational methods

	Solvent	H2	H3	H4	H5	H6	OH	Subst.
[1] Phenol	$CDCl_3$	6.826	7.240	6.928	7.240	6.826	4.692	
	CHARGE	6.843	7.212	6.917	7.212	6.843	4.704	
	GIAO[a]	6.897	7.388	7.014	7.388	6.897	3.781	
	GIAO[b]	6.672	7.163	6.789	7.163	6.672	3.556	
	ACD	6.750	7.110	6.800	7.110	6.750	8.500	
	DMSO	6.750	7.152	6.760	7.152	6.750	9.287	
[2] 2-Fluorophenol	$CDCl_3$		7.060	6.845	7.010	7.010	5.077	
	CHARGE		6.959	6.931	6.980	6.858	4.957	
	GIAO[a]		7.231	6.882	7.180	7.254	4.715	
	ACD		6.980	7.090	6.760	7.240	5.550	
	DMSO		7.103	6.762	6.956	6.956	9.725	
[3] 2-Chlorophenol	$CDCl_3$		7.310	6.864	7.175	7.014	5.508	
	CHARGE		7.207	6.877	7.178	6.913	5.616	
	GIAO[a]		7.393	6.924	7.307	7.191	5.018	
	ACD		6.980	7.090	6.760	7.240	5.550	
	DMSO		7.306	6.788	7.129	6.957	10.061	
[4] 2-Bromophenol	$CDCl_3$		7.455	6.804	7.217	7.019	5.470	
	CHARGE		7.372	6.832	7.193	6.918	5.459	
	GIAO[a]		7.504	6.926	7.344	7.249	5.156	
	ACD		7.470	6.760	7.200	6.990	8.350	
	DMSO		7.456	6.724	7.170	6.946	10.144	
[5] 2-Iodophenol	$CDCl_3$		7.658	6.680	7.247	6.999	5.281	
	CHARGE		7.551	6.624	7.130	6.843	5.005	
	GIAO[a]		6.942	6.467	6.807	6.904	4.407	
	ACD		7.590	6.610	7.170	6.940	10.950	
	DMSO		7.658	6.583	7.190	6.884	10.278	
[6] 2-Methylphenol	$CDCl_3$		7.114	6.842	7.076	6.761	4.604	2.250
	CHARGE		7.019	6.860	7.023	6.743	4.525	2.294
	GIAO[a]		7.306	6.958	7.161	6.594	3.827	2.325
	ACD		6.990	6.720	6.930	6.590	5.100	2.180
	DMSO		7.032	6.669	6.967	6.753	9.153	2.092
[7] 2-Methoxyphenol	$CDCl_3$		6.850	6.850	6.850	6.911	5.590	3.886
	CHARGE		6.686	6.811	6.802	6.709	5.570	3.782
	GIAO[a]		6.670	6.900	7.051	7.115	5.310	3.908
	ACD		6.790	6.780	6.840	6.860	5.720	3.830
	DMSO		6.750	6.750	6.750	6.900	8.823	3.750
[8] 2-Cyanophenol	$CDCl_3$		7.511	7.000	7.478	6.998	5.659	
	CHARGE		7.539	7.175	7.496	7.119	5.567	
	GIAO[a]		7.601	7.033	7.595	7.233	5.441	
	ACD		7.480	7.430	7.480	7.010	6.160	
	DMSO		7.581	6.921	7.485	7.009	11.024	
[9] 2-CF_3-phenol	$CDCl_3$		7.510	7.008	7.422	6.955	5.440	
	CHARGE		7.746	7.113	7.432	7.089	5.295	
	GIAO[a]		7.705	7.259	7.652	7.087	5.649	
	ACD		7.570	7.220	7.330	7.040	6.880	
	DMSO		7.491	7.020	7.442	6.919	10.454	
[10] 2-Nitrophenol	$CDCl_3$		8.094	6.973	7.565	7.144	10.555	
	CHARGE		8.090	7.233	7.577	7.176	10.387	
	GIAO[a]		8.423	6.925	7.634	7.322	11.498	
	ACD		8.020	6.970	7.550	7.140	10.620	
	DMSO		7.875	6.978	7.543	7.134	10.890	
[11] Methyl salicylate	CDCl3		7.833	6.873	7.449	6.978	10.727	3.949
	CHARGE		7.898	7.135	7.388	7.047	10.756	3.894
	GIAO[a]		8.085	6.877	7.547	7.150	11.078	3.914

DOI: 10.1002/mrc

Table 3. (*Continued*)

	Solvent	H2	H3	H4	H5	H6	OH	Subst.
	ACD		7.800	6.880	7.460	6.970	10.690	3.980
	DMSO		7.786	6.948	7.524	6.988	10.485	3.898
[**19**] 2-hydroxybenzaldehyde	CDCl3		7.567	7.027	7.535	6.997	11.024	9.903
	CHARGE		7.678	7.161	7.520	7.066	11.101	9.893
	DMSO		7.666	6.964	7.522	6.999	10.685	10.258
[**20**] 2-hydroxyacetophenone	CDCl3		7.730	6.896	7.466	6.972	12.242	2.627
	CHARGE		7.617	7.165	7.511	7.083	12.305	2.665
	DMSO		7.890	6.963	7.532	6.958	11.954	2.641

[a] CH_4 as reference using B3LYP-6−311++g(d,p), for both optimization and GIAO calculation.
[b] C_6H_6 as reference using B3LYP-6−311++g(d,p), for both optimization and GIAO calculation.

Table 4. ^{1}H chemical shifts (δ) of *para* substituted phenols in $CDCl_3$ and DMSO together with calculated chemical shifts using various computational methods

	Solvent	H2,6	H3,5	OH	Subst.
[**12**] 4-Cyanophenol	$CDCl_3$	6.917	7.556	5.266	
	CHARGE	7.116	7.592	5.095	
	GIAO[a]	6.867	7.663	4.203	
	ACD	6.920	7.530	6.300	
	DMSO	6.903	7.630	10.583	
[**13**] 4-Fluorophenol	$CDCl_3$	6.763	6.921	4.604	
	CHARGE	6.878	7.013	4.450	
	GIAO[a]	6.783	7.056	3.688	
	ACD	6.720	6.920	8.500	
	DMSO	6.736	6.969	9.313	
[**14**] 4-t-bu-phenol	$CDCl_3$	6.749	7.252	4.557	1.290
	CHARGE	6.817	7.082	4.540	1.380
	GIAO[a]	6.764	7.337	3.652	1.291
	ACD	7.090	7.060	5.470	1.350
	DMSO	6.668	7.159	9.064	1.224
[**15**] 4-Nitrophenol	CDCl3	6.898	8.157	5.356	
	CHARGE	7.183	8.083	5.334	
	GIAO[a]	6.829	8.476	4.428	
	ACD	6.920	7.530	6.300	
	DMSO	6.948	8.117	10.997	
[**16**] 4-CF_3-phenol	CDCl3	6.896	7.509	5.050	
	CHARGE	7.024	7.683	4.842	
	GIAO[a]	6.910	7.713	4.185	
	ACD	6.970	7.260	8.150	
	DMSO	6.921	7.519	10.243	
[**17**] 4-Methoxyphenol	$CDCl_3$	6.758	6.791	4.521	3.759
	CHARGE	6.748	6.757	4.364	3.766
	GIAO[a]	6.587	6.986	3.397	3.741
	ACD	6.830	6.800	9.570	3.800
	DMSO	6.670	6.738	8.848	3.652

	Solvent	H2	H3	H4	H5	H6	OH	Subst.
[**18**] 2,4-Chlorophenol	$CDCl_3$		7.324		7.150	6.950	5.466	
	CHARGE		7.227		7.195	6.890	5.562	
	GIAO[a]		7.458		7.209	7.101	5.065	
	ACD		7.280		7.110	6.920	5.550	
	DMSO		7.432		7.199	6.967	10.442	

[a] CH_4 as reference using B3LYP-6−311++g(d,p), for both optimization and nmr calculation.

DOI: 10.1002/mrc

is −0.08, −0.09 and −0.17 ppm for the *ortho*, *meta* and *para* protons, respectively. The observed long range effect on the *para* proton may be due to a change in the π-electron distribution. This possibility was investigated by calculating the π-excess on the aromatic carbons with and without the influence of the DMSO molecule. The calculations were performed using DFT at the B3LYP/3−21G level of theory and the results are given in Table 5.

The differential π-electron excess (leading to the π-shift) on the *para* proton is significant and corresponds to a change in the chemical shift of 0.11 ppm which agrees with the observed shielding of 0.17ppm. The change of π-shift at the *ortho* carbon is more difficult to interpret since a direct interaction with the DMSO molecule may be involved.

Using semi-empirical models, such as those in the CHARGE programme, specific interactions must be recognized and treated separately. In this treatment,[45] the predicted $\Delta\delta$ values for phenol are 4.57 (OH) and 0.00, −0.08, −0.08 for the *ortho*, *meta* and *para* protons which are all in good agreement with the observed values. These effects have been incorporated in the CHARGE programme so that solvent specific calculations can be made; however these results are reported elsewhere[45] and shall not be further discussed here.

Chemical shift calculation

In order to calculate the chemical shifts reported in Tables 3 and 4 using the CHARGE programme, it is necessary to include the two effects mentioned previously for the OH chemical shift. These are the π-shift contribution through the oxygen atom and the effect of close proximity of the substituent in the intramolecularly H-bonded systems.

π-shift contribution through oxygen

In the CHARGE programme, the π-shift contribution to the ^{1}H chemical shift of a proton attached to an aromatic carbon atom (i.e. H−C_{AR}) has been obtained from NMR experiments as 10 ppm/electron.[43] The effect of π density on the oxygen atom over the OH chemical shifts can now be obtained from the data given for the 4-substituted phenols in dilute solution using π electron withdrawing or donating substituents. The *para* substituted compounds are ideal as the *meta* substituents have little π effect on the OH group and the *ortho* substituents have more contributions than merely π effects.

Table 6 gives the OH proton chemical shift *versus* the excess π-electron density on the oxygen atom as calculated by CHARGE. There is a linear correspondence with a coefficient of 42.3 ppm/π electron. This when inserted into the CHARGE programme gives the calculated shifts in Table 6. The coefficient for oxygen is *ca* 4 times that for carbon. Interestingly, this value is nearly identical to that for the nitrogen atom in anilines (42.7 ppm/el) from a similar correlation for *para* substituted anilines.[47] Thus, one 2p-electron pair on the X atom in a X−H bond is sufficient to produce this effect.

Table 5. The differential π-excess (me) on the ring carbons of phenol, with and without interaction with DMSO

	Phenol	Phenol + DMSO	Δ(π-excess)
Ipso	−3.4	7.9	11.3
Ortho	−70.6	−71.9	1.3
Meta	9.7	3.4	6.3
Para	−36.0	−47.1	11.1

H-bonding contributions to the OH chemical shift

In previous investigations on *ortho* substituted phenols with strong intramolecular H-bonds (e.g., 2-hydroxybenzalde hyde) with OH···O=C distances <2.0 Å, the large deshielding effect of the *ortho* substituent on the OH proton was modelled in CHARGE by a r^{-12} function Eqn (2) which when added to the other contributions gave good agreement with the observed shifts.[36] Eqn (2) applies only for $r < 2.0$ Å, since the CHARGE calculations beyond this point are represented well with the current model.

$$\delta_{HB} = [(2/r)^{12} - 1]/2 \quad (2)$$

In the compounds considered here, the *ab initio* calculations show clearly that the OH shielding is a *linear* function of the H···O distance for $r < 2.1$ Å. It is also dependant on the H···O=C−R dihedral angle φ. Thus we require an equation of the form of Eqn (3) for our calculations.

$$\delta_{HB} = [A + B(r - r_0)] \quad \cos^2\varphi \quad (3)$$

The slope of the plot (*B*) is given by the *ab initio* calculations as −7.6 ppm/Å. It is of interest to note that if the two observed OH shifts for 2-hydroxybenzaldehyde **19** and 2-hydroxyacetophenone **20** (Table 3) are used with the *ab initio* H···O distances, the value for the slope *B* is −7.8 ppm/Å, in complete agreement with the theoretical value above. Thus, this value is adopted for all the functional groups considered here. The curve in Fig. 4 for acetone is a $\cos^2\varphi$ function and thus the hydrogen-bonding term is maximum when the H···O=C−R entity is planar and $\varphi = 0$ or 180° and decreases to zero as the dihedral angle approaches 90 degrees. This value is set to zero at this angle since the calculated decrease in the nuclear shielding (*ca* 3 ppm *cf*. Figure 4) corresponds closely to the magnitude of the hydrogen-bonding term needed when using the default contributions included in CHARGE. However, in all the compounds considered here the H···O=C−R entity is

Table 6. The OH proton chemical shift of *para* substituted phenols *versus* the excess π-density (me) on the oxygen atom

Para subst.	Exp.	π-dens	Calcd
NO_2	5.356	120.4	5.334
CN	5.266	115.0	5.095
CF_3	5.050	109.5	4.842
H	4.692	107.2	4.704
F	4.604	100.1	4.561
t-Bu	4.557	103.1	4.540
OMe	4.521	98.5	4.364

DOI: 10.1002/mrc

planar, thus the $\cos^2\varphi$ dependence cannot be experimentally verified.

The values of A and r_0 were found to be zero and 2.05 Å for all the strong intramolecular hydrogen bonds studied, that is with nitro, aldehyde, ketone and ester groups. In methyl salicylate, the large steric coefficient of the CO oxygen was reduced for these short distances, but no other change was needed in the calculation. Thus, this equation may be applied to any functionality capable of forming such hydrogen bonds.

The chemical shifts for all the phenols shown in Tables 3 and 4 were calculated using the CHARGE programme modified as described and the ACD and *ab initio* GIAO calculations. These were plotted against the observed chemical shifts and are shown in Fig. 7. The slope, intercept and the correlation coefficients of these plots are given in Eqn (4).

$$\begin{aligned}
\delta_{\text{observed}} &= 0.993\delta_{\text{calculated}} + 0.059, \quad R^2 = 0.994, \quad \text{CHARGE} \\
\delta_{\text{observed}} &= 0.869\delta_{\text{calculated}} + 1.043, \quad R^2 = 0.965, \quad \text{GIAO} \\
\delta_{\text{observed}} &= 1.462\delta_{\text{calculated}} - 2.421, \quad R^2 = 0.947, \quad \text{ACD} \qquad (4)
\end{aligned}$$

The CHARGE calculations reproduce the experimental data well. The *ortho* substituted compounds not involved in strong intramolecular hydrogen bonds (OH···O distance >2 Å) have not been used in the parameterization of the CHARGE programme and serve as an objective basis for comparison with other chemical shift calculation methods and to determine the general accuracy of the programme.

In Fig. 7, there are a number of outliers in the OH region (4–6 ppm) for the ACD calculated chemical shifts. These outliers are likely to be due to averaging of $CDCl_3$ and DMSO data. The corresponding correlation coefficient is therefore very poor. If all the OH protons are excluded, there is much better agreement ($R^2 = 0.982$). There are also discrepancies around this region from the GIAO calculations and this may be due to the exclusion of solvent effects in these calculations, and again an improved correlation is found when the OH protons are removed ($R^2 = 0.982$). The CHARGE data correlates well in this region and when the OH data is removed, the correlation coefficient is hardly affected($R^2 = 0.996$).

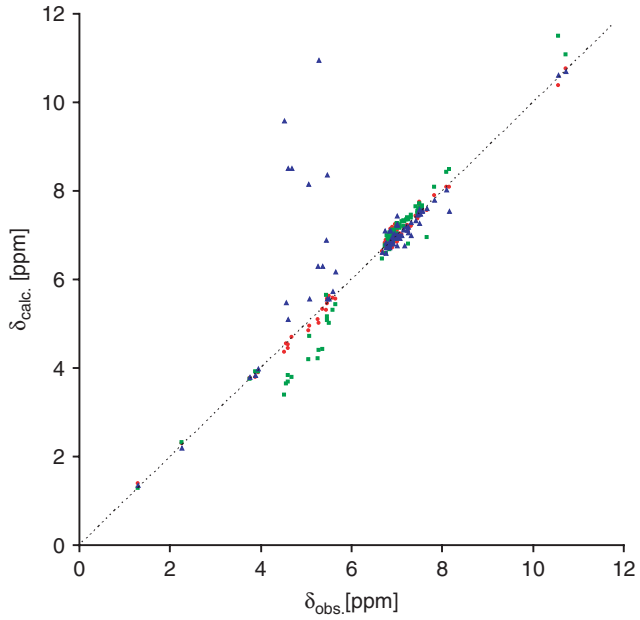

Figure 7. Calculated *versus* observed chemical shifts (CHARGE = red circles, GIAO = green squares, ACD = blue triangles).

In general, we note that the ACD predictions are often extreme in that when they are correct they are very accurate but when erroneous rather large errors are found. This is to be expected as data, which is well represented in the database in the correct solvent, will be reproduced accurately whilst poorly represented data is likely to contain large errors. The GIAO data contains much fewer outliers; however, the data seems to follow a trend which is slightly tilted compared to the diagonal. This kind of superimposed trend had been observed before[33,48] and may be due to inaccuracies in the DFT calculations and/or the exclusion of solvent effects.

The importance of solvent specific chemical shift calculations is apparent from the data presented here. The solvent effects found for the OH protons are present for all the proton chemical shifts but to a varying extent. These effects are not important for ^{13}C chemical shifts since often the ^{13}C nuclei are not in direct contact with the solvent molecules. This is one of the major reasons (another being the rather narrow chemical shift range of protons) why less success has been achieved in predicting ^1H chemical shifts using either database or *ab initio* calculations whereas the same methods have been successfully applied to ^{13}C chemical shift predictions.

The results show that atoms in the vicinity of hydroxyl protons have a large effect on their chemical shifts. By elucidating the OH oxygen π-shift, the CHARGE programme can accurately model these non-bonded effects for atoms farther than 2 Å from the OH proton. The classical models of anisotropy, steric, and electric field incorporated in the programme, however were initially found to fail in describing the chemical shifts of OH protons closer than 2 Å to a carbonyl oxygen atom. This interaction was identified as a strong hydrogen-bonding interaction and has been corrected for by the introduction of an additional term which was parameterized using *ab initio* DFT calculations.

The analysis undertaken here was carried out on phenols, however since the effect of conjugation is treated separately and parameterized separately it should not affect calculations of non-conjugated systems. Furthermore, the theoretical analysis on the geometrical effects of a carbonyl group strongly hydrogen bonding with OH protons should be equally applicable to any OH protons even though the system studied here was an OH proton in a phenol. However, as detailed elsewhere[40] the geometrical effects of an oxygen atom (or indeed any other nuclei) which is not sp^2 hybridized (such as the oxygen atom in the DMSO molecule) may vary and thus the ^1H chemical shift calculations of strongly hydrogen-bonded OH protons in the CHARGE programme are only applicable to cases where the acceptor atom is an sp^2 hybridized oxygen atom. Thus, this hydrogen-bonding term must be separately parameterized for systems not containing sp^2 hybridized oxygen atoms. Fortunately in organic

DOI: 10.1002/mrc

chemistry and particularly in biologically relevant systems, the carbonyl oxygen is by far the most common hydrogen bond acceptor in strong hydrogen bonds (closer than 2 Å).

CONCLUSIONS

Hydrogen bonding in phenols has been studied using NMR, IR and theoretical calculations. Classical models incorporated in the CHARGE programme have been used to calculate the chemical shift of the OH proton of phenols. The acidity of the OH proton was revealed to be a significant factor in determining the self-association of phenols. This interaction could be directly observed on the IR spectrum and confirmed by observing the ^{1}H shifts with different concentrations. The drastic change in OH proton chemical shift and IR frequency when the proton is brought within 2 Å of an electronegative atom is remarkable. Here, classical models fail to describe the observed chemical shift, and an additional correction term is needed. In these cases, it is likely that the orbital overlaps are such that a bonding orbital is formed whereas what we have so far viewed as weak hydrogen bonding only reflect the stabilizing interaction of opposite charges. This explanation is consistent with the observed experimental results, and hence it is not surprising to find the classical models for chemical shifts to be inaccurate. Therefore, a correction based on these findings was introduced and parameterized using experimental and *ab initio* data.

It was shown that the hydrogen bonding of DMSO with phenol has a large effect on the OH chemical shifts and a significant effect on the electronic configuration of phenol. The chemical shift of the *para* proton in phenol was shown to be due to π-electron density changes resulting from the interaction with DMSO. In addition to the correction for molecules involved in strong intramolecular hydrogen bonding, a correction was made to determine the effect of the π-electron excess on the oxygen atom on the chemical shift of an attached proton. The coefficient was much larger than that for a C–H atom and very similar to that for an NH atom. The chemical shifts, as calculated by the CHARGE model, were compared with calculations from other chemical shift calculation approaches. The results showed very consistent chemical shift calculations using CHARGE whether the OH protons were included or not. The GIAO and ACD calculations are significantly improved when the OH protons are removed. The ACD calculations are poor for the OH protons as these seem to be calculated as an average of $CDCl_3$ and DMSO data.

Although it would be ideal from a practical point of view to combine molecular mechanics with CHARGE calculations to predict chemical shifts, one should take especial care in cases where strong hydrogen bonding occurs, since the force field would have to produce hydrogen-bond lengths with an accuracy within fractions of an angstrom, in order to calculate the chemical shifts accurately. Unless the force fields used can reproduce such high accuracy, one should use the resulting chemical shift calculations as rough estimates (indeed, for binding studies such estimates may still be of great interest). Conversely, this means that one may use experimental data to extract hydrogen bond distances with equally high precision.

EXPERIMENTAL

All the compounds were obtained commercially (Sigma-Aldrich). The solvents, obtained commercially, were stored over molecular sieves and used without further purification. ^{1}H and ^{13}C NMR were obtained on a Bruker Avance spectrometer operating at 400 MHz for proton and 100 MHz for carbon. HSQC and HMBC experiments were also performed. Fluorine decoupled proton spectra were obtained at GSK Stevenage at 500 MHz for the fluorinated compounds. ^{1}HNMR spectra at 700 MHz were recorded for 2- and 4-methoxyphenol. Typical running conditions (^{1}H spectra) were 128 transients, spectral width 5000 Hz and 32K data points zero-filled to 64 k. The 2D experiments were conducted using the standard Bruker pulse sequences. The spectra were recorded in 10 mg/ml solutions (^{1}H) and *ca* 30 mg/ml (^{13}C) in $CDCl_3$ and d_6-DMSO with a probe temperature of *ca* 300 K and referenced to TMS. The IR spectra of the compounds were recorded at 10 mg/ml concentration using $CDCl_3$ as solvent to retain the same conditions as the ^{1}H NMR spectra. At 10 mg/ml, little or no intermolecular hydrogen bonding is observed in the IR spectrum in $CDCl_3$ except for 2- and 4-cyanophenol (**8** and **12**) and 4-nitrophenol (**15**). In these compounds, high self-association was observed and these spectra were obtained at 1 mg/ml and their OH chemical shifts treated separately. The IR spectra were run on a Perkin-Elmer 883 spectrometer operating in the double beam mode with 1 cm optical length quartz cells with NaCl windows. $CDCl_3$ solvent was used as reference. All spectra were recorded at room temperature.

Computational

The geometries were minimized using Gaussian98,[29] at the B3LYP/6–311++G(d,p) level. For post third row atoms, this basis set is insufficient and the recommended[49] basis set LANL2DZ was used. As noted previously,[50] this basis set produces very poor results. The geometry used for 2-iodophenol was that of 2-bromophenol replacing the bromine atom with an iodine atom and using the experimental I–C bond length. The GIAO calculations were performed using DFT (B3LYP) with the 6–311++G(d,p) basis set as recommended[31] for H-bonded systems, for all but the iodo compound, where the LANL2DZ basis set was used. ACD data base calculated values were obtained using the ACD/HNMR predictor v. 5.[51] It should be noted that revised versions of the ACD software have been presented after the preparation of this manuscript. The new revisions may perform better as solvent effects are one of the updated features. This shows the direction of progress in this field and has no impact on the interpretation of the results presented here. All calculations were performed on a PC.

Spectral assignments

Phenol and 2-substituted phenols

The assignments of the ring protons were straightforward and agreed with the additive SCS tables found

DOI: 10.1002/mrc

in the literature.[1] The ^{13}C data in the literature for 2-bromophenol[52,53] were contradictory, so the assignment was made and confirmed with an HMQC experiment. This agreed with data from A. Brossi *et al*.[53] The complex patterns of 2-fluorophenol and 2-methylphenol (*o*-cresol) were assigned by HMQC experiments and the known ^{13}C shifts.[54]

The spectrum of 2-methoxyphenol (guaiacol) gave a complex splitting pattern at 400 MHz. The literature ^{13}C data[55] was inconclusive, thus the carbon assignment was confirmed and the proton chemical shifts assigned from HMQC and HMBC experiments.

The spectrum of 2-cyanophenol was assigned using proton, carbon, HMQC and HMBC experiments. The ^{13}C spectrum in DMSO had been assigned[52] but was reassigned and the correct carbon data is as follows (in $CDCl_3$). ^{13}C: C1,159.043; C2, 99.807; C3, 135.182; C4, 121.335; C5, 133.309; C6, 117.047; CN, 116.731.

4-substituted phenols

For 4-cyano, 4-fluoro and 4-t-Bu-phenol, the assignmemts were obvious. In 4-methoxy phenol, the ring protons are close together and the assignment from SCS tables was uncertain, thus HMQC and HMBC experiments were used to assign the proton spectra.

2,4-dichlorophenol

The previous assignment[34] for this compound in $CDCl_3$ was confirmed and used. The observed chemical shifts in $CDCl_3$ and DMSO solution are given in Tables 2 and 5, with previous data for 2-hydroxybenzaldehyde **19** and 2-hydroxy acetophenone **20** from Abraham *et al*.[36]

Acknowledgements

We thank the EPSRC and GSK for a CASE research studentship (M.M.) and GSK for the 500 MHz spectra of the fluorinated compounds. We also thank Drs. Richard Smith and Ben Bardsley at GSK for their valuable contribution and technical support and R.J.A acknowledges the award of an Emeritus Leverhulme Fellowship.

REFERENCES

1. Abraham RJ, Fisher J, Loftus P. *Introduction to NMR Spectroscopy* (2nd edn). John Wiley & Sons: Chichester, UK, 1988.
2. Pretsch E, Sibl J, Clerc T. *Determination of Organic Compounds* (2nd edn). Springer–Verlag: London, 1989.
3. Kishi Y. *Tetrahedron* 2002; **58**: 6239.
4. Schlecht MF. *Molecular Modeling on the PC*. John Wiley & Sons: New York, 1998.
5. Saunders M, Houk KN, Wu Y, Still WC, Lipton M, Chang G, Guida WC. *J. Am. Chem. Soc.* 1990; **112**: 1419.
6. Modgraph Consultants. NMRPredict, 2.14.0, http://www.modgraph.co.uk/, 2004.
7. Laatikainen R. *Perch*. Perch Solutions: Kuopio, 2007.
8. Ghanty TK, Staroverov VN, Koren PR, Davidson ER. *J. Am. Chem. Soc.* 2000; **122**: 1210.
9. Dannenberg JJ, Haskamp L, Masunov A. *J. Phys. Chem. A* 1999; **103**: 7083.
10. Abraham RJ. *Prog. Nucl. Magn. Reson. Spectrosc.* 1999; **35**: 85.
11. Pauling L. *J. Chem. Phys.* 1936; **4**: 673.
12. Zumwalt LR, Badger RM. *J. Am. Chem. Soc.* 1940; **62**: 305.
13. Baker AW. *J. Am. Chem. Soc* 1958; **80**: 3598.
14. Abildgaard J, Bolvig S, Hansen PE. *J. Am. Chem. Soc.* 1998; **120**: 9063.
15. Tribble MT, Traynham JG. *J. Am. Chem. Soc.* 1961; **62**: 305.
16. Merril JR. *J. Am. Chem. Soc.* 1961; **65**: 2023.
17. Liddel U, Becker ED. *Spectrochim. Acta* 1957; **10**: 70.
18. Kuhn LP. *J. Am. Chem. Soc.* 1951; **74**: 2492.
19. Davies M. *Trans. Faraday Soc.* 1938; **34**: 1427.
20. Davies M. *Trans. Faraday Soc.* 1940; **36**: 1114.
21. Clausser WF, Wall FT. *J. Am. Chem. Soc.* 1939; **61**: 2679.
22. Vinogradov SN, Linnell RH. *Hydrogen Bonding*. Van Nostrand Reinhold: New York, 1971.
23. Hibbert F, Emsley J. *Adv. Phys. Org. Chem.* 1990; **26**: 255.
24. Liddle U, Becker ED. *Spectrochim. Acta* 1957; **1957**(10): 70.
25. Porte AL, Gutowsky HS, Hunsberger IM. *J. Am. Chem. Soc.* 1960; **82**: 5057.
26. Davis JC, Deb KK. *Adv. Magnet. Res.* 1970; **4**: 201.
27. Seguin J, Guillaume-Vilport F, Uzan R. *J. Chem. Soc., Perkin Trans. 2* 1986; 773.
28. Simperler A, Lambert H, Mikenda W. *J. Mol. Struct.* 1998; **448**: 191.
29. Frisch MJ, Trucks GW, Schlegel HB, Scuseria GE, Robb MA, Cheeseman JR, Zakrzewski VG, Montgomery JA, Stratmann RE, Burant JC, Dapprich S, Millam JM, Daniels AD, Kudin KN, Strain MC, Farkas O, Tomasi J, Barone V, Cossi M, Cammi R, Mennucci B, Pomelli C, Adamo C, Clifford S, Ochterski J, Petersson GA, Ayala PY, Cui Q, Morokuma K, Malick DK, Rabuck AD, Raghavachari K, Foresman JB, Cioslowski J, Ortiz JV, Baboul AG, Stefanov BB, Liu G, Liashenko A, Piskorz P, Komaromi I, Gomperts R, Martin RL, Fox DJ, Keith T, Al-Laham MA, Peng CY, Nanayakkara A, Challacombe M, Gill PMW, Johnson B, Chen W, Wong MW, Andres JL, Gonzalez C, Head-Gordon M, Replogle ES, Pople JA. *Gaussian 98, Revision A9*. Gaussian: Pittsburg, 1998.
30. Espinosa E, Souhassou M, Lachekar H, Lecomte C. *Acta Crystallogr. B* 1999; **55**: 563.
31. Lipowski P, Koll A, Karpfen A, Wolschann P. *Chem. Phys. Lett.* 2002; **360**: 256.
32. Grabowski SJ. *J. Mol. Struct.* 2001; **562**: 137.
33. Lampert H, Mikenda W, Karpfen A, Kählig H. *J. Phys. Chem. A* 1997; **101**: 9610.
34. Bagno A. *Chem. Eur. J.* 2001; **7**: 1652.
35. Abraham RJ, Canton M, Edgar M, Grant GH, Haworth IS, Hudson BD, Mobli M, Perez M, Smith PE, Reid M, Warne MA. *Charge7*. University of Liverpool: Liverpool, 2004.
36. Abraham RJ, Mobli M, Smith RJ. *Magn. Reson. Chem.* 2003; **41**: 26.
37. Dingley AJ, Grzesiek S. *J. Am. Chem. Soc.* 1998; **120**(33): 8293.
38. Barfield M. *J. Am. Chem. Soc.* 2002; **124**: 4158.
39. Mayo SL, Olafson BD, Goddard WAG III. *J. Phys. Chem.* 1990; **94**(26): 8897.
40. Mobli M. 1H NMR calculation and modelling of organic molecules, PhD Thesis, University of Liverpool, Liverpool, 2004.
41. Ishikawa R, Kojima C, Ono A, Kainosho M. *Magn. Reson. Chem.* 2001; **39**: S159.
42. Abraham RJ, Canton M, Reid M, Griffiths L. *J. Chem. Soc., Perkin Trans. 2* 2000; 803.
43. Günther H. *NMR Spectroscopy* (2nd edn). John Wiley & Sons: Chichester, UK, 1995.
44. Griffiths VS, Socrates G. *J. Mol. Struct.* 1966; **21**: 3.2.
45. Abraham RJ, Byrne JJ, Griffiths L, Perez M. *Magn. Reson. Chem.* 2006; **44**: 491.
46. Salman SR, Kudier AR. *Spectrochim. Acta* 1990; **46A**(8): 1147.
47. Abraham RJ. *Personal Communication*. University of Liverpool: Liverpool, 2004.
48. Abraham RJ, Mobli M, Smith RJ. *Magn. Reson. Chem.* 2004; **42**: 436.
49. Foresman JB, Frisch AE. *Exploring Chemistry with Electronic Structure Methods* (2nd edn). Gaussian: Pittsburgh, 1996.
50. Abraham RJ, Bardsley B, Mobli M, Smith RJ. *Magn. Reson. Chem.* 2004; **42**: 436.
51. Williams A, Bakulin S, Golotvin S. *NMR Prediction Software, 5.0*. Advanced Chemistry Development: Toronto, Ontario, 2001.
52. Smith WB, Proulx TW. *Org. Magn. Reson.* 1976; **8**: 567.

53. Brossi A, Hsu F, Rice KC, Rozwadowska MD, Schmidhammer H, Hufford CD, Chiang CC, Karle IL. *Helv. Chim. Acta* 1981; **64**(5): 1672.
54. Rae ID, Weigold JA, Kowalewski DG, Biekofsky RR, Contreras RH. *Magn. Reson. Chem.* 1996; **34**(3): 181.
55. Malterud KE, Anthonsen T. *Acta Chem. Scand.* 1987; **B 41**: 6.

DOI: 10.1002/mrc